Draft version July 8, 2019
Preprint typeset using LaTeX style AASTeX6 v. 1.0

ENHANCING WFIRST SCIENCE WITH THE ADDITION OF A REDDER FILTER

George Helou, John Stauffer, J. Davy Kirkpatrick, Peter Capak, Lee Armus, Kirsten Larsen, Sean J. Carey (Caltech/IPAC), Robert A. Benjamin (U. Wisconsin-Whitewater), Massimo Marengo (Iowa State U.), Jacob Jencson, Mansi Kasliwal (Caltech), James M. Bauer (U. Maryland), Dante Minniti (U. Andres Bello, Chile), John Bally (U. Colorado), Nicolas Lodieu (Instituto de Astrofisica de Canarias), Brendan P. Bowler (U. Texas-Austin), ZengHua Zhang (Nanjing U. and Obs. de Paris), Stefanie Milam (GSFC), Bryan Holler (STScI), Adam Burgasser (UC San Diego), S. T. Megeath, J. D. Smith (U. Toledo)

ABSTRACT

WFIRST will be capable of providing Hubble-quality imaging performance over several thousand square degrees of the sky. The wide-area, high spatial resolution survey data from WFIRST will be unsurpassed for decades into the future. With the current baseline design, the WFIRST filter complement will extend from the bluest wavelength allowed by the detector response to a reddest filter (F184W) that has a red cutoff at 2.0 microns. In this white paper, we outline a number of science advantages for adding a K_s filter ($\lambda_c \sim 2.15$ μm), and propose to extend the wavelength coverage for WFIRST into the K-band, where the gains of going to space are much more pronounced than at shorter wavelengths.

1. INTRODUCTION

WFIRST was the top priority of the National Academy of Sciences' 2010 Decadal Survey for Astronomy and Astrophysics. Its design has been optimized to conduct groundbreaking studies of dark energy and exoplanet demographics. Those dark energy and exoplanet research programs are enabled by WFIRST's wide-field camera which will provide imaging with HST sensitivity and spatial resolution over an instantaneous field of view that is nearly two orders of magnitude larger. While the majority of the observing time during WFIRST's prime mission will be devoted to the core dark energy and exoplanet microlensing surveys, about 25% of the observing time is being set aside for community-specified and peer-reviewed Guest Observer (GO) programs. The ability of WFIRST to address the most diverse and exciting science at the time of the mission would be greatly enhanced by providing a long wavelength filter that is centered as far to the red as allowed by the telescope and detector design.

Compelling science enabled by such a red filter ranges from Solar System studies to the search for earliest galaxies. We discuss some of these science topics below in order to motivate the recommendation that a filter be added to the Wide Field Instrument (WFI) on WFIRST. This addition is proposed in the context of the Decadal Survey Scope which states that "the study may include findings and recommendation regarding those plans (referring to WFIRST, Athena and LISA), as appropriate, including substantive changes in NASA's plans."

2. DISCOVERY SPACE ADVANTAGE OF A K FILTER

The deepest, wide-area K-band survey of the sky is the VISTA VHS survey (Banerji et al. 2015), now nearing completion. The VHS covers the entire southern sky to a depth of about $K(\mathrm{Vega}) = 18$ mag, 5σ. As demonstrated in the Appendix, a K_s filter on WFIRST could obtain survey data to a depth that is more than five magnitudes deeper than the VHS. Using the same exposure times and dithering strategy as for the planned WFIRST high-latitude survey, the WFIRST survey speed to this depth will be about 20 square degrees per day per filter. No other existing or planned wide-area survey could come anywhere close to imaging such large areas to these faint limits at this wavelength.

There is no viable replacement for the kind of very deep, wide-field K band imaging that WFIRST could provide. WFC3 on HST does not go longward of H band; neither does EUCLID. Technical, not scientific, considerations, drove the decision to exclude a K-band filter in both of these missions: thermal emission from the optics would have badly degraded performance at those wavelengths. The baseline plan for WFIRST is that it will be operated at about 260K, cold enough to allow efficient use of a K-band filter. Over the past year, on-going design and analysis work has led to improved performance margins, including reduced WFI thermal background, implying even better sensitivity than shown in Table 1 of this paper. It is technically feasible and scientifically compelling to take advantage of the first cool, wide-field telescope in space by providing WFIRST with the reddest possible filter.

As can be seen in Figure 1, the advantage of WFIRST over ground increases by 100× (5 mag) at K_s (*vs* VHS) as the wavelength drops below $1\mu m$ (*vs* LSST). All of the benefits of a redder filter described here rely on a *relatively* cold operating temperature and the stable

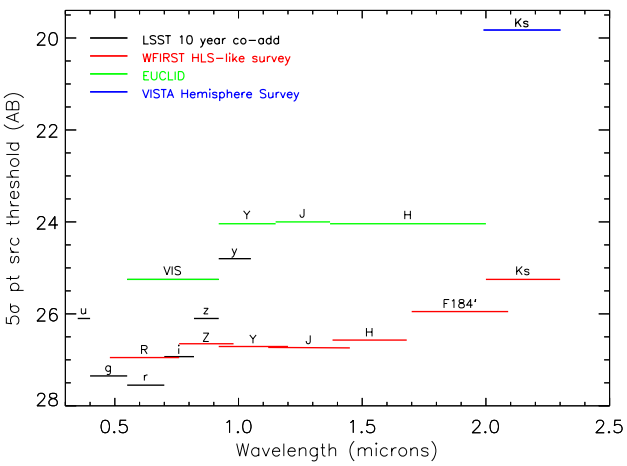

Figure 1. Comparison of the sensitivities of WFIRST, Euclid and LSST, along with VISTA-VHS. The LSST values are for the full 10 year co-add data at the end of the survey. WFIRST limits are for its High Latitude Survey (HLS), or an analogous observing pattern at the other wavelengths, namely R, Z and K_s. We estimated the depths at the latter bands by scaling from the Y, J, H and F184 depths by relative sensitivities. The sensitivity for our proposed K_s filter is shown in the figure based on an assumed telescope temperature of 260 K (the F184 filter sensitivity is also for that assumed temperature).

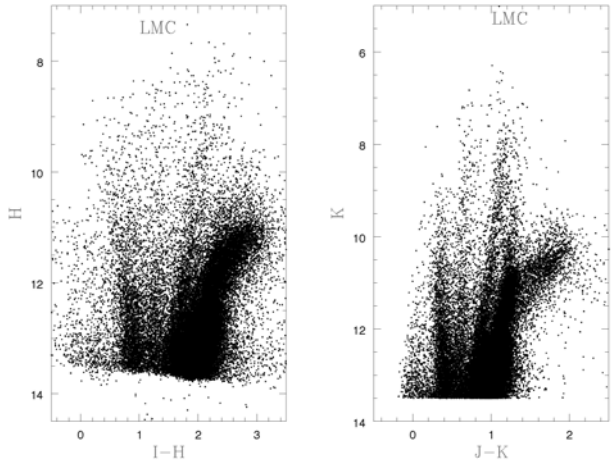

Figure 2. Two versions of the color-magnitude diagram for giant stars in the LMC, one utilizing $I-H$ for the x-axis and one using $J-K$. The same stars are plotted in the two panels. The $J-K$ diagram clearly sharpens the distinction between different sequences, particularly for carbon stars (the finger pointing up and to the right for $J-K>1.4$, and oxygen rich supergiants (the narrow finger extending above the giant branch, beginning at $J-K=1.2$ and $K=10.5$). The stars plotted are those in the Spitzer SAGE (Meixner et al. 2006) LMC survey; we have cross-matched those stars to the 2MASS and SDSS databases. See Boyer et al. (2011) for a discussion of the post-main sequence demographics that can be distinguished if a K filter is available.

PSF, small pixel size and accurate photometry that will be available at L2 even if the sensitivity is not limited by natural backgrounds. Moreover, the addition of a K_s filter would make WFIRST more consistent with the Decadal recommendation for a *near-infrared* telescope.

There are simple astrophysical arguments why a redder filter would open up important new regions of discovery space. For giants, IR colors that include a K band are optimal for separating populations (see Nikolaev & Weinberg 2000 and Figure 2). The H^- opacity minimum (and Rayleigh-Jeans spectra) results in stars with a very broad range of spectral types and luminosities having very similar H-K colors; the range from types B to K is less than 0.2 magnitudes. This means that this color can be used to estimate extinction when it is large, with relatively small errors (see §3). Similarly, the strong molecular bands in brown dwarfs result in their J-K color providing a means to accurately estimate their metallicity, making it possible for WFIRST to identify and characterize the substellar population of the thick disk and halo better than any other facility (see §5). Finally, accurate distances to RR Lyrae stars (to map the structure of tidal streams in the MW or as the first rung of a Pop II distance ladder) is best done with WFIRST with a K filter - the Period-Luminosity (PL) relation is shallower (or non-existent) at shorter wavelengths and both extinction and metallicity effects are lower at K than at shorter bands. We address specific science enabled by a redder filter in more detail in the next several sections.

3. THE IMF AT VERY LOW MASS

The Stauffer et al. Science White Paper submitted to the Decadal Survey (Number 108) describes the unique advantages of a deep K-band imaging survey with WFIRST for this topic.

4. STRUCTURE AND KINEMATICS OF THE MW BULGE, NUCLEAR CLUSTER AND INNER DISK

The inner 3 kpc region of our galaxy is much more complex than once thought. The existence of a strong bar was first recognized more than 25 years ago (Blitz & Spergel 1991); Spitzer IRAC data (Benjamin et al. 2005) and ground-based NIR data (Wegg et al. 2015) have recently provided much improved maps of the extent and orientation of the bar. The shape of the bulge is tri-axial rather than spheroidal, resulting in an X-shaped or boxy appearance (Ness & Lang 2016). Most of the mass in the bulge resides in a relatively metal rich (Fe/H ~ -0.5 to 0), rotationally supported population which traces the bar. However, a minority "hot" (high RMS velocity, low rotation), more spheroidal, more metal poor population (Fe/H ~ -1) is also present (Dekany et al. 2013, Gran et al. 2016). Finally, there is possible evidence for a young population interior to the 3 kpc arm which may have more disk-like structure, possibly containing up to 10% of the bulge mass (Portail et al. 2016).

While there has been much progress in the past decade, observations of the bulge and bar from the

ground are inherently difficult due to the large extinction towards the galactic center. Going into the infrared can remove much of the obscuring effects of the dust, but then the limitation becomes the high stellar source density encountered in the central regions. WFIRST with the reddest possible filter would offer the best means to enable new research. Figures 3 and 4 illustrate the advantages of redder filters and smaller PSFs for studies of the inner disk and bulge.

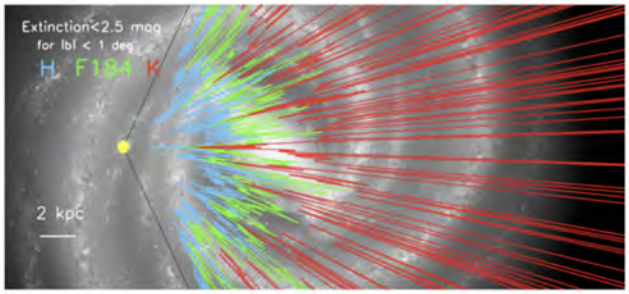

Figure 3. The extinction "horizon" in the H, F184 and K band, i.e. the distance where $A_{band} > 2.5$, as a function of Galactic longitude superimposed on an "artist's conception" of the Milky Way Galaxy by Robert Hurt. This uses the three-dimensional dust extinction model of Marshall et al (2006). At each longitude slice, we plot the distance corresponding to the maximum extinction at that wavelength for any latitude value. Note the volume of the Galaxy with modest (less than a factor of ten) extinction expands dramatically by going to the K band. Going to the K-band allows us to probe directly the farthest reaches of the galaxy and map the outer spiral arms.

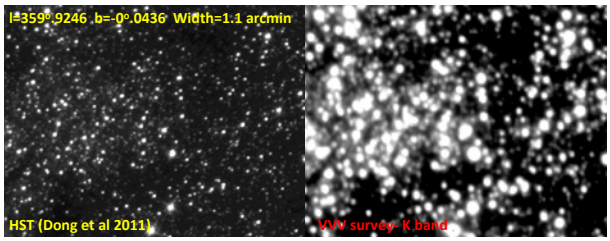

Figure 4. A comparison of a small pointing (1.1 arcmin in width) near the Galactic center. The left panel shows a HST F190 (1.9 μm) image from Dong et al (2011); the right panel shows a ground-based K_s image from the VVV survey (Minniti et al 2010). Note the dark areas in both images due to high extinction clouds toward the Galactic center. With a K-filter, WFIRST would have the best of both programs: the ability to see through a higher dust column in the K-band *combined* with spectacular angular resolution.

One example of new science enabled by a wide-area H/K or J/K survey of the bulge with WFIRST would be a much more detailed map of the spatial distribution of red-clump giants (tracers of the metal rich bulge population) than possible from the ground, definitively measuring the orientation, length, and width of the bar and plausibly allowing one to trace whether spiral arms originate from the ends of the bar. A more demanding role for WFIRST, but one that could provide unique and far-reaching new data, would be to obtain several epochs of that map at K over the 5-year WFIRST prime mission, or better yet over an extended mission timeframe. Such data, when combined with the dense astrometric grid expected from Gaia, could provide proper motions for tens to hundreds of thousands of red-clump giants and thousands of RR Lyr stars, thereby providing kinematic data needed to help empirically constrain the origins and evolution of the metal poor and metal rich populations of the inner galaxy (100 km/s at 8.5 kpc corresponds to about 2.4 mas/yr), as well as providing constraints on the relative contributions of dark and luminous matter in the inner Galaxy. There are plans already to use data from the 2.8 square degrees of the microlensing campaigns to address these questions. A GO program that provided H/K-band imaging of significantly more sight-lines through the bulge and inner disk, particularly where extinction limits sensitivity at shorter wavelengths, could not be obtained by any other facility and would greatly improve the results from the planned microlensing survey.

Another specific project would be to obtain synoptic K band imaging of the inner ∼30' of the Galaxy (four WFI fields) in order to identify all of the RR Lyrae stars in the Nuclear Star Cluster (NSC) and Nuclear Bulge/disk. A dozen or so RR Lyr have recently been identified in the NSC using HST and data from the VVV survey (Dong et al. 2017; Minniti et al. 2016); however, those surveys are very incomplete due to the extreme crowding and variable reddening (see Figure 4). Yet determination of the total number of RR Lyr in the NSC is vital for constraining its formation mechanism. Is most of the mass of the NSC from the merger of a previous generation of globular clusters (Tremaine et al. 1975) or from in-situ star-formation (Agarwal & Milosavljevic 2011)? A survey with WFIRST (single epoch at J band, multi-epoch at K band) would be the best way to identify the complete RR Lyr population of the NSC and much of the Nuclear Bulge and thereby answer that question. The same data could be used to measure the proper motions of these RR Lyr and thereby determine their kinematics.

5. USING A K FILTER ON WFIRST TO PROVIDE A NEW H_0 DISTANCE LADDER

The most accurate current cosmic distance ladders to determine the value of the Hubble constant are based, respectively, on data primarily at J and H bands (Riess et al. 2011) and at IRAC [3.6] and [4.5] micron bands (Freedman et al. 2012). The fact that the HST ladder did not use K band was not because K band is disfavored for some astrophysical or cosmological reason, but simply because the thermal operating temperature of HST greatly reduces its sensitivity at that wavelength. All of the primary initial rungs used in such distance ladders (Cepheids, RR Lyr variables, TRGB) work better at longer wavelengths because the longer wavelengths are less affected by reddening and metallicity variations. If HST had the same thermal environment as now ex-

pected for WFIRST, WFC3 would have had a K filter and the HST distance ladder would very likely have used K band data.

In order to construct a PopII distance ladder (Beaton et al. 2016), accurate RR Lyrae distances require a well defined PL relation. Differently than for Cepheids, this relation exists only at long wavelengths. For short wavelengths the slope of the PL relation is just too shallow, and the intrinsic scatter too large (>5%), to produce accurate distances. The rapid increase in the slope of the PL relation happens in the near-IR, where the intrinsic scatter due to evolutionary effects and temperature dependence is greatly reduced because of a narrowing in the instability strip and because the brightness variations are mainly driven by radius changes. In fact, RR Lyrae distances in the K band are as accurate as the distances that can be derived in the L and M bands, with just a small penalty for the larger extinction at K compared to L or M. The accuracy in the distances obtained in the J and H bands will instead be lower, not just because of the higher extinction, but also because of the larger intrinsic scatter in the PL relation (in the V band there is no PL relation). The distances obtained in the K band are very accurate even for individual stars: these variables can therefore be used to probe the geometry of the host galaxies, in addition to anchoring the distance scale.

Given the importance of reconciling the tension between the measured local value of H_0 and the large-scale value of H_0 inferred from CMB data (Bernal et al. 2016, Riess et al. 2011), it seems likely that JWST will be used to produce a new distance ladder. In the absence of a true K band filter, the most efficient way for JWST to obtain high precision distances of RR Lyrae in Local Group galaxies will be to use the NIRCam F200W or F277W wide filters (best for reducing crowding), in addition to the Spitzer/IRAC-like F356W and F444W passbands (where the extinction is even lower). For most of these galaxies however, the small size of NIRCam detectors will limit these observations to narrow areas in each galaxy, a limitation that does not exist with the huge WFIRST field of view. A survey of these extended targets with WFIRST in the K band would enable efficient sampling of a much larger population of RR Lyrae than is feasible with JWST, reducing the scatter in their PL relation due to the metallicity dispersion within those galaxies, providing more accurate anchors for the JWST PopII distance scale. By observing these fields with both F184W and a K_s filter, synthesized WFIRST magnitudes closely matched to the F200W bandpass could be produced, allowing the WFIRST and JWST data to be precisely aligned.

6. IDENTIFYING AND CHARACTERIZING INFRARED TRANSIENTS WITH WFIRST

In addition to the survey science potential, a K-band filter on WFIRST would make for a powerful and unique capability for Time-Domain Astronomy (TDA) in the near-infrared. It would go much deeper than ground-based K-band surveys, much deeper than LSST on a visit-by-visit basis and therefore for the same cadence, and much deeper (5mag) than Spitzer. WFIRST would also offer much better spatial resolution than LSST or Spitzer, a critical advantage for exploring the transient source populations in more crowded parts of galaxies. Two examples of science applications of this TDA capability are discussed below, but the most recent illustration comes from the first detection of electromagnetic counterparts to gravitational waves from neutron star mergers; by 10 days after its discovery, the peak of the SED of the Neutron Star-Neutron Star merger event GW 170817 had shifted to 2.1 μm (Pian et al. 2017). This was predicted by Kasen et al. (2013) and Barnes & Kasen (2013) who showed that the peak of the emission is beyond 1.4μm due to the large number of line transitions in heavy elements produced by r-process nucleosynthesis. More recent opacity calculations (Fryer et al., in prep.) suggest that the emission could be even redder and even fainter than initially predicted.

The Spitzer Infrared Intensive Transients Survey (SPIRITS) has recently uncovered a population of transients that show predominantly (and often exclusively) infrared emission (see Kasliwal et al. 2017). These transients, dubbed Especially Red Intermediate Luminosity Transient Events (SPRITEs), lie in the luminosity gap between novae and supernovae and photometrically evolve on a wide range of timescales. Half a dozen have been discovered in nearby galaxies surveyed by SPIRITS out to 7 Mpc, but they would be easily detected by WFIRST at K-band out to ∼100 Mpc. The much larger sample that could be discovered by WFIRST would provide the data necessary to firmly identify the progenitor types and physical mechanisms which give birth to the SPRITES. Current possible interpretations of SPRITEs include formation of massive star binaries, stellar mergers, birth of stellar mass black holes, electron capture supernovae on extreme AGB stars, etc. Since the emission from SPRITEs peaks in the mid-IR, with T_{eff} between 350 and 1000 K, a redder WFIRST filter would be much more sensitive to discovering and characterizing these events. Moreover, without a K-band filter to establish colors, the most interesting SPRITEs may go unidentified as such, even if detected at optical wavelengths.

A WFIRST galactic plane survey would provide the first epoch data needed to identify and characterize the explosive events in high-mass star-forming regions that we have only recently begun to detect (Bally et al. 2015; Caratti o Garatti et al. 2017; Hunter et al. 2017). These events have been found in very crowded, heavily embedded regions, requiring good spatial resolution and the longest wavelength filters possible. Do young high mass stars grow primarily from mergers or from intermittent, high accretion rate bursts from their circumstellar disks? A K-band enabled WFIRST could best help provide the data to answer that question. When the next Type II

supernova occurs in the Milky Way, this same WFIRST galactic plane survey could provide the data needed to characterize the progenitor of that event.

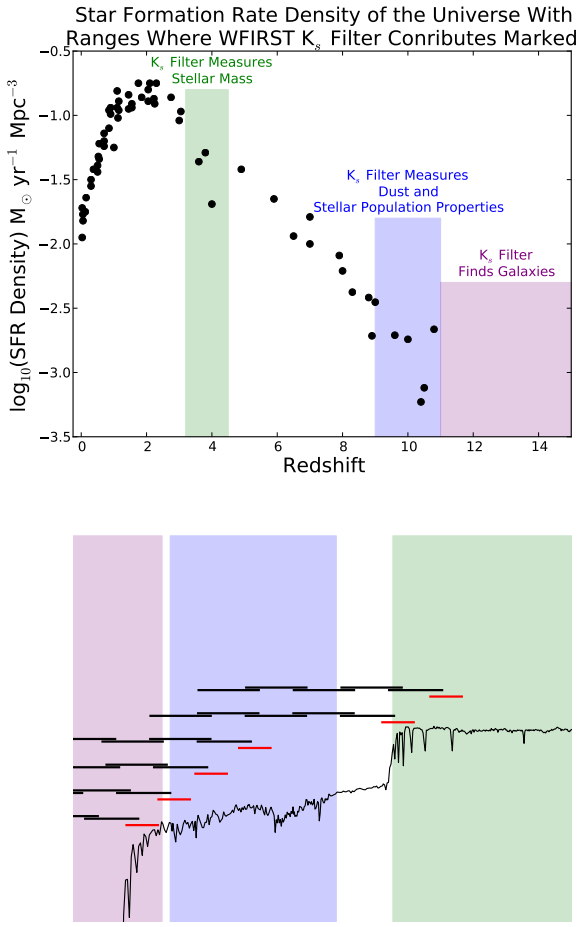

Figure 5. **Left:** The global history of the star formation rate density is shown using the compilation from Madau & Dickinson (2014) with updated $z > 8$ points from Ishigaki et al. (2018). A K_s band filter on WFIRST would make several key contributions to understanding the rise in the global star formation rate at $z > 3$. First, indicated in green, it would enable stellar mass estimates at $3.5 < z < 4.5$, as galaxies were approaching their maximum star formation rate. Second, indicated in blue, it would enable estimates of the ultraviolet spectral slope at $9 < z < 11$ which is a crucial period for changes in the intrinsic stellar population and dust content of galaxies. Finally, indicated in purple, it would enable searches for $11 < z < 15$ galaxies which JWST does not have the survey speed to find (see Figure 6). **Right:**The rest frame Spectral Energy Distribution (SED) of a 100Myr old galaxy is shown along with regions where a WFIRST K_s band filter would contribute information. The region of the SED probed by WFIRST filters at different redshifts is indicated in black for the existing Z, Y, J, H, F184 filters and red for the proposed K_s filer. The rest frame optical, indicated in green, contains information on the stellar mass and age of galaxies. The 1500-3000Å ultraviolet portion of the SED indicated in blue contains information on the intrinsic hardness of the ultraviolet radiation and the dust content of galaxies. Finally, the Ly-α break at 1216Å allows one to select galaxies at $11 < z < 15$.

7. IMPROVING EXTRAGALACTIC POPULATION STUDIES AT $Z > 3$

Extragalactic surveys would benefit in several ways from extending the WFIRST wavelength coverage beyond $2\mu m$. The left hand panel of Figure 5 shows current measurements of the global star formation history along with regions where a WFIRST K_s band would add critical information. First, as shown in the right hand panel of Figure 5, a K_s-band survey on WFIRST would extend the redshift range for which stellar masses can be estimated from z $\sim$ 3.5 to z $\sim$ 4.5. This enables one to probe beyond the peak of the global star formation at z $\sim$ 2-3 (Madau & Dickinson 2014). The combination of sensitivity and area that WFIRST could provide compared to ground based and existing Spitzer surveys would enable studies of early dwarf galaxy formation linked to dark matter formation via galaxy clustering measurements (Lee et al. 2012, 2009, Finkelstein et al. 2015). This co-measurement of clustering and galaxy mass provides a strong constraint on the duty cycle and possible star formation histories in the early universe (Lee et al. 2009, Finkelstein et al. 2015).

Second, the addition of a longer-wavelength filter would significantly improve the selection efficiency of 9 $<$ z $<$ 11 galaxies and enable measurements of their rest-frame UV spectral slopes, which are very sensitive to their evolving stellar populations and dust content (Finkelstein et al. 2012, Madau and Dickinson 2014, Figure 5).

Finally, as shown in Figures 5 and 6 the longer wavelength lever arm could also be used to find 11 $<$ z $<$ 15 galaxies if they exist (Madau and Dickinson 2014), a task that only a many square degree WFIRST deep field could address due to the limited survey speed of JWST (Yung et al. 2018, Mashian et al. 2016). Such a deep survey would also find heavily obscured super-starbursts at z $>$ 4 (Caputi et al. 2012, Wang et al. 2012), which are also very faint and rare on the sky.

Another key advantage of a red filter for extra-galactic science is the ability to find and differentiate quasars from stars and galaxies to low luminosities, which is difficult without longer-wavelength IR data (Masters et al. 2012, Figure 7). It appears that the population of very massive black holes that form quasars is dropping rapidly at z $>$ 6 (e.g. Banados et al. 2016; Mazzucchelli et al. 2017). The ability to measure the upper envelope of the quasar luminosity function to z $\sim$ 10 combined with fainter quasars at lower redshifts will place strong constraints on early black hole formation models.

8. CHARACTERIZING WATER ICE ON DISTANT SOLAR SYSTEM OBJECTS WITH WFIRST

A K-band filter, particularly a K_s-band filter, can facilitate searches for volatiles on the surfaces of the outer solar system small bodies (Figure 8; Trujillo et al. 2011). Both planned and possible GO large-area surveys (e.g. HLS) will yield imaging data that will contain many small bodies, and those with apparent slower

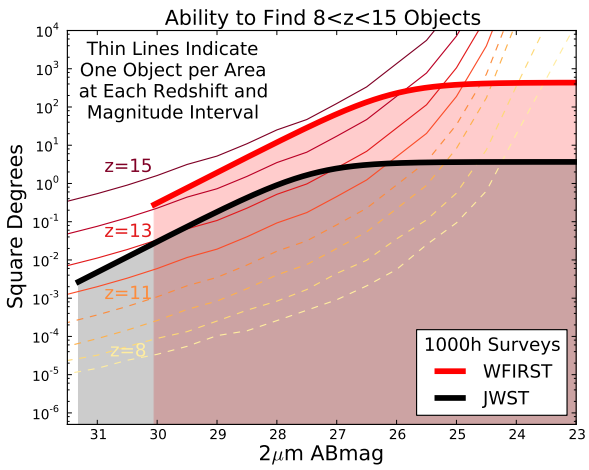

Figure 6. The thick red and black lines show the depth and area reachable by WFIRST and JWST in 1000h respectively. A given 1000h survey would be one point on the line and probe areas and depths smaller than the point. For WFIRST we assumed a survey in 5 filters (Y,J,H,F184W, K_s) and used the current overhead estimates provided by C. Hirata (private communication). For JWST we assumed a 3 filter (F115W, F150W, F200W) NIRCAM survey with the actual overheads given by the Astronomers Proposal Tool (APT) excluding the 0.5h slew to field overhead. Galaxies were assumed to be 0.1″ FWHM gaussians when estimating sensitivity. The area where one object is expected in a given survey per magnitude and redshift interval is indicated with thin dashed lines for redshift ranges accessible with the existing WFIRST filter complement and solid lines for redshift ranges only reachable if WFIRST had a K_s band filter. With these filters JWST would not be able to select $z < 9$ galaxies due to the lack of Y band data. The lines are based on models of measured data at $8 < z < 10$ from Yung et al. (2018). At $11 < z < 15$ the $z = 10$ Yung et al. (2018) estimate is scaled by the density evolution of dark matter given in Mashian et al. (2016). The error on the density in these models is $\pm 0.2 - 0.5$ dex due to a combination of current measurement error, cosmic variance, and the assumptions in the extrapolations.

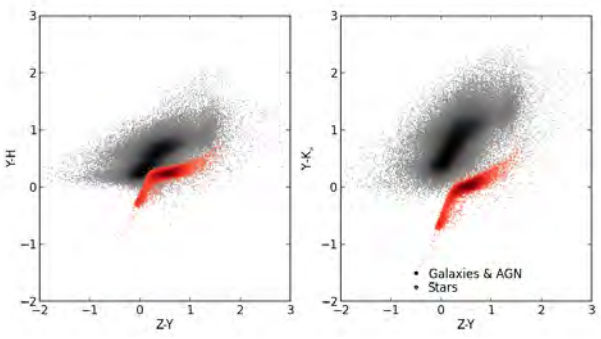

Figure 7. Adding a K_s band to WFIRST (right), increases the separation between stars (red) and other objects (black) compared with the H band (left) allowing for clear differentiation between stars and other objects. Actual data from the COSMOS (Laigle et al. 2016) catalog are shown using HST F814W as a stand in for WFIRST Z band and Ultra-Vista Y, H, and K_s bands. The star/galaxy separation in this plot is based on HST F814W morphology along with the Laigle et al. (2016) catalog.

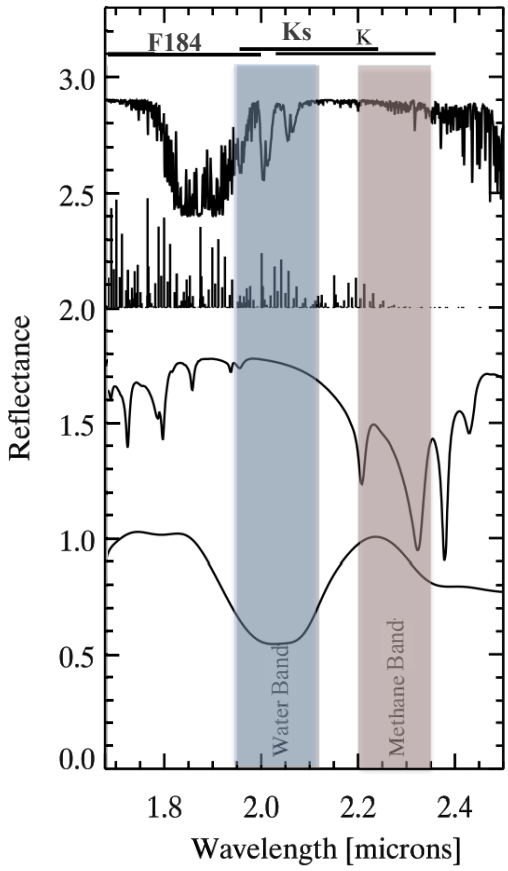

Figure 8. As adopted from Trujillo et al. (2011), a K or Ks band filter would provide a direct measure of water and methane absorption.

non-sidereal motions, i.e. the outer solar system small bodies, Centaurs and Trans-Neptunian Objects (TNOs), will have only slightly elongated images in ~ 3 minute medium-deep exposures, thus minimizing confusion and read-noise effects due to trailing. These TNOs and Centaurs are also the most likely bodies to have detectable surface water ice, since most or all of them will have formed beyond the "snow line" where the water-ice sublimation rate rapidly drops off (c.f. Dones et al. 2015). Furthermore, because within that population the larger objects are more likely to have retained their surface volatiles since their formation (Schaller & Brown 2008), it is likely that it is the brighter objects which will manifest water ice features.

While not exclusively within the water-ice band at 2-μm, a strong absorption feature would dominate the Ks band, relative to the Y, J and F184 bands which should be unaffected by strong water-ice absorption. Adding Ks-band imaging to such wide-area surveys would allow identification of potentially hundreds of icy outer-solar system bodies, with the brightest TNOs or Centaurs being promising targets for follow-up spectral observations with JWST or other future facilities. The surveys themselves would place meaningful constraint on the ubiquity

of water ice among the TNO and Centaur populations.

9. TECHNICAL DISCUSSION

Figure 9 shows the wavelength coverage by the current set of filters baselined for WFIRST, and the effective collecting area of the optical and detector system within each filter. The significant drop towards the blue within the R-band filter is primarily due to a decrease in detector responsivity. Not shown is a potential K-band filter, which would benefit from the detectors' performance continuing flat out to $2.5\mu m$. The defining science goals of the mission require filters Y, J, H and W, whereas filters Z and R were added mainly for their potential benefit to the Guest Observer program. This is reflected in the choice of camera pixel size at $0.11arcsec$, which runs from $2\lambda/D$ at R to $0.6\lambda/D$ at K.

WFIRST will deliver greater depth and resolution than larger ground-based survey telescopes at all wavelengths, but that advantage improves dramatically beyond $1\mu m$, as can be seen in Figure 1. One value added by the filters in common between WFIRST, Euclid and LSST is the ability to cross-calibrate the surveys with limited recourse to astrophysical source modeling. That cross-survey calibration however can be achieved with sufficient accuracy by anchoring it to one or two bands in common, since each survey has its own requirements on cross-band calibration. Finally, adding a K band filter to WFIRST will enhance the complementarity between Euclid and WFIRST spectral coverage.

The WFIRST Project is best placed to address the technical options for adding a K band filter to WFI and their associated cost. While we do not attempt to estimate the cost here, we do believe it is very modest in view of the compelling scientific gains across a vast range of astrophysics achievable with a K band capability.

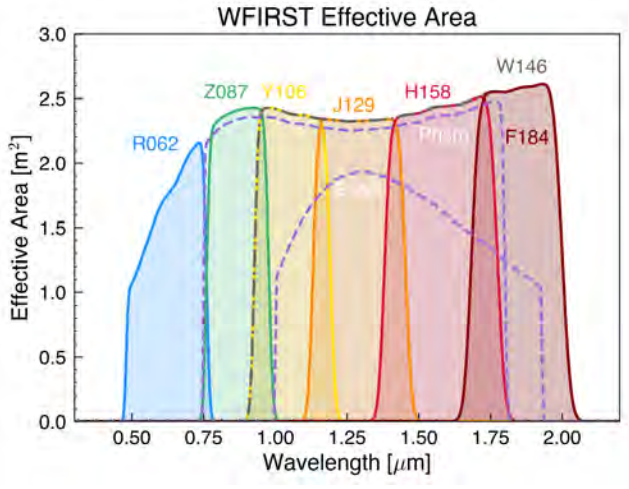

Figure 9. Current baseline WFIRST filter set, showing the effective area at each wavelength. The drop towards the blue within R062 is due primarily to the drop in detector responsivity. By contrast, the detector cutoff at the red end is around $2.5\mu m$.

10. SUMMARY AND CONCLUSIONS

The discovery space opened up by a redder WFIRST filter is huge, and there is no forseeable alternative source for a comparable K-band deep/wide survey capability. We are confident the community would find myriad ways to exploit that discovery space, and we encourage the Decadal Committee to consider the science opportunity cost of flying WFIRST without such a filter, and to recommend a modest extension of WFIRST to longer wavelengths.

REFERENCES

Agarwal, M. & Milosavljevic, M. 2011, ApJ, 729, 35.
Allard, F., Homeier, D., & Freytag, B. 2014, Astronomical Society of India Conference Series, 11, 33.
Bally, J., Ginsburt, A., Silvia, D. et al. . 2015, A&A, 579, 130.
Banados, E., Venemans, B., Decarli, R. et al. . 2016, ApJS, 227, 11.
Baraffe, I., Homeier, D., Allard, F., & Chabrier, G. 2015, A&A, 577, A42.
Barnes, J. & Kasen, D. 2013, ApJ, 775, 18.
Banerji, M., Jouvel, S., Lin, H. et al. . 2015, MNRAS, 446, 2523.
Beaton, R., Freedman, W., Madore, B. et al. 2016, ApJ, 832, 210.
Benjamin, R., Churchwell, E., Babler, B. et al. 2005,ApJ, 630, 149.
Bernal, J., Licia, V., & Riess, A. 2016, JCAP 10, 019.
Blitz, L. & Spergel, D. 1991, ApJ, 379, 631.
Blum, R., Mould, J., Olsen, K. et al. 2006, AJ, 132, 2034.
Borysow, A., Jorgensen, U. G., & Zheng, C. 1997, A&A, 324, 185.
Bowler, B., Liu, M., Mawet, D. et al. 2017, AJ, 153, 18.
Boyer, M., Girardi, L., Marigo, P. et al. 2013, ApJ, 774, 83.
Caputi, K., Dunlop, J., McLure, R. 2012, ApJ, 750, 20.
Caratti o Garatti, A., Stecklum, B., Garcia Lopez, R. et al. 2017, NatPh 13, 276.
Cutri, R. M., Wright, E. L., Conrow, T., et al. 2013, Explanatory Supplement to the AllWISE Data Release Products (wise2.ipac.caltech.edu/docs/release/allwise/expsup/).
Davidge, T., Olsen, K., Blum, R. et al. 2005, AJ, 129, 201.
Dong, H., Wang, Q., Cotera, A. et al. 2011, MNRAS, 417, 114.
Dong, H., Schodel, R., Williams, B. et al. 2017, MNRAS, 471, 3617.
Dekany, I., Minniti, D., Catelan, M. et al. 2013, ApJL, 776, L19.
Dones, L., Brasser, R., Nathan, K., & Rickman, H. 2015, SSRv, 197, 191.
Finkelstein, S., Papovich, C., Salmon, B. et al. 2012, ApJ, 756, 164.
Finkelstein, S., Song, M., Behroozi, P. et al. 2015, ApJ, 814, 95.
Freedman, W., Madore, B., Scowcroft, V. et al. 2012, ApJ, 758, 24.
Gran, F., Minniti, D., Saito, R. et al. 2016, A&A, 591, 145.
Hunter, T., Brogan, C., MacLeod, G. et al. 2017, ApJ, 837, L29
Ishigaki, M., Kawamata, R., Ouchi, M. et al. 2018, ApJ, 854, 73.
Kahn, S. 2016, presentation to AAAC, Jan. 29, 2016.
Kasen, D., Badnell, N., & Barnes, J. 2013, ApJ, 774, 25.
Kasliwal, M., Bally, J., Masci, F. et al. 2017, arXiv:1701.01151.
Kirkpatrick, J. D., Kellogg, K., Schneider, A. C., et al. 2016, ApJS, 224, 36.
Kirkpatrick, J. D., Schneider, A., Fajardo-Acosta, S., et al. 2014, ApJ, 783, 122.
Lee, K.-S., Giavalisco, M., Conroy, C. et al. 2009, ApJ, 695, 368.
Lee, K-S., Ferguson, H., Wiklind, T. et al. 2012, ApJ, 752, 66.
Kunder, A., Rich, R., Koch, A. et al. 2016, ApJ, 821, L25.
Laigle, C., McCraken, H. J., Ilbert, O. et al. 2016 ApJS, 224, 24.
Lodieu, N., Hambly, N., Jameson, R. et al. 2007, MNRAS, 374, 372.
Lodieu, N., Dobbie, P., Cross, N. et al. 2013, MNRAS, 435, 2474.
Madau, P. & Dickinson, M. 2014, ARAA, 52, 415.
Marshall, D., Robin, A., Reyle, C. et al. 2006, A&A, 453, 635.
Mashian, N., Oesch, P., & Loeb, A. 2016, MNRAS, 455, 2101.
Masters, D., Capak, P., Salvato, M. et al. 2012, ApJ, 755, 169.
Mazzucchelli, C., Banados, E., Venemans, B. et al. 2017, ApJ, 849, 91.
Meixner, M., Gordon, K., Indebetouw, R. et al. 2006, AJ, 132, 2268.
Minniti, D., Lucas, P., Emerson, J. et al. 2010, NewAstronomy, 15, 433.
Minniti, D., Saito, R., Gonzalez, O. et al. 2014, A&A, 571, A91.
Minniti, D., Contreras Ramos, R., Zoccali, M. et al. 2016, ApJ, 830, L14.
Ness, M. & Lang, D. 2016, AJ, 152, 14.
Nikolaev, S. & Weinberg, M. 2000, ApJ, 542, 804.
Perez-Villegas, A., Portail, M., & Gerhard, O. 2017, MNRAS, 464, L80.
Pian, E., D'Avanzo, P., Benetti, S. et al. 2017, arxiv 1710.05858.
Portail, M., Ortwin, G., Wegg, C., & Ness, M. 2016, arxiv 1608.07954.
Riess, A., Macri, L., Casertano, S. et al. 2011, ApJ, 730, 119.
Riess, A., Casertano, S., Yuan, W. et al. 2019, ApJ, 876, 85.
Romualdez, L., Benton, S., Clark, P. et al. 2016, arxiv 1608.02502.
Schaller, E. L. & Brown, M. E. 2008. ApJ, 659, L61.
Tremaine, S., Ostriker, J., & Spitzer, L. 1975. ApJ, 196, 407.
Trujillo, C. A., Sheppard, S. S. & Schaller, E. L. 2011. ApJ, 730, 105.
Wang, W-H., Barger, A., & Cowie, L. et al. 2012, ApJ, 744, 155.
Wegg, C., Gerhard, O. & Portail, M. 2015, MNRAS, 450, 4050.
Yung, L., Somerville, R., Finkelstein, S. et al. 2018, arxiv 1803.09761.
Zhang, Z., Pinfield, D., Galvez-Ortiz, M. et al. 2017, MNRAS, 464, 3040.
Zhang, Z., Homeier, D., Pinfield, D., et al. 2017, MNRAS, 468, 261.
Zhang, Z.H., Galvez-Ortiz, M.C., Pinfield, D.J., et al. 2018, MNRAS, 480, 5447.
Zoccali, M., Vasquez, S., Gonzalez, O. et al. 2016, arxiv 1610.09174.

APPENDIX

Table 1 provides estimated WFIRST sensitivities for a filter similar to the 2MASS K_s filter, for three possible operating temperatures (J. Kruk, private communication). This table was built over a year ago to illustrate the value of a filter at $\lambda > 2\mu m$ regardless of the uncertain temperature of the telescope. In fact the design has now converged at the lowest temperature (column in boldface) and even lower temperature for the baffles, further improving the performance of such a filter.

Table 1. S/N Achieved as a Function of K_s-band mag in an HLS Survey

K_s mag (AB)	K_s mag (Vega)	T=260K	T=270K	T=284K
18.00	16.15	**946.1**	930.9	879.5
18.50	16.65	**754.4**	727.0	668.0
19.00	17.15	**584.7**	562.7	497.9
19.50	17.65	**455.5**	430.2	362.6
20.00	18.15	**351.3**	323.3	257.3
20.50	18.65	**267.3**	237.8	178.0
21.00	19.15	**199.6**	170.6	120.2
21.50	19.65	**145.7**	119.2	79.6
22.00	20.15	**103.7**	81.3	51.9
22.50	20.65	**71.9**	54.2	33.5
23.00	21.15	**48.6**	35.6	21.4
23.50	21.65	**32.2**	23.0	13.6
24.00	22.15	**21.1**	14.8	8.7
24.50	22.65	**13.6**	9.4	5.5
25.00	23.15	**8.7**	6.0	3.5
25.5	23.65	**5.5**	3.8	2.2

[a] Assumes five exposures with a total observing time of 868 s. For K_s band, m(AB) − m(Vega) = 1.85. Zodiacal level set at 1.44 times the minimum.